R.E.M. (Rekayasa Energi Manufaktur) Jurnal | Vol.11 No.2/2026
ISSN online (2528-3723)
http://doi.org/10.21070/rem.v11i2.1856

Thermo-hydraulic Performance of Double-cut and Perforated Twisted Tape Based on Constant Surface Area

Naufal Faizurrahman Siregar[1], Damora Rhakasywi[2*], Nicky Yongkimandalan[3]
[*]Email corresponding author: rhakasywi@upnvj.ac.id

[1,2,3]Mechanical Engineering Department, Faculty of Engineering, Universitas Pembangunan Nasional Veteran Jakarta

Article history: Received: 1 Juni 2026 | Revised: 3 Juli 2026 | Accepted: 6 Juli 2026

Abstract*. Improving the heat transfer of the heat exchanger pipe is necessary. Inserting twisted tapes is often applied because it increases the Nusselt number, but it causes excessive pressure drop. This study investigates three variations of twisted tape, namely: plain, semicircular double cut, and circular perforation. The research gap concerns reducing the surface area of the twisted tape to the same area. Simulation using ANSYS Fluent. Variation analysis shows the Nusselt number increased by 36.64% for smooth, 40.94% for double semicircular cuts, and 36.95% for circular perforations. The friction factor increased by 232.26%, 253.46%, and 239.96%, respectively. The PEC value for each variation below 1 indicates a decrease in efficiency after the addition of the twisted tape. However, this study concludes that the double cut has the highest efficiency compared to other variations for the Reynolds number range of 6000 to 17000.*

Keywords – *Twisted tape; nusselt number; friction factor.*

INTRODUCTION

The performance of heat exchanger tubes is crucial across industries such as power generation, oil and gas processing, cooling, heating, ventilation, and air conditioning (HVAC), and petrochemicals. Therefore, efforts to improve heat exchanger performance are necessary. Many investigations have been carried out to enhance the thermal transfer efficiency of tubes used in heat exchangers [1]. One effective approach is to disrupt the fluid flow, thereby increasing heat transfer through forced convection. Adding twisted tape components inside the heat exchanger tube can create disturbances or turbulence in the fluid flow, thereby enhancing heat transfer. Twisted tapes are often used due to their simple design and relatively easy installation. However, the addition of twisted tapes may also enhance the friction factor, consequently lowering the pressure loss in the fluid movement [2] [3].

. The twisted tape modifications used in this study are semicircular double-cut and circular perforated. The research process uses CFD software, namely ANSYS FLUENT, to simulate heat transfer under various flow conditions and heat exchanger designs. The simulation results are presented as the Nusselt number (Nu) and the friction factor (f) [4][5]. Each of these values represents the increase in convective heat transfer and the increase in the friction factor in the flow that causes the pressure drop. The calculation of the Performance Evaluation Criteria (PEC) value is required to assess work efficiency by balancing the benefits of increased heat transfer against the pressure-drop losses [8].

Several previous studies have modified the twisted tape component. The most commonly used modifications are cutting and perforating. One of the previous studies that carried out cutting modifications [7] used double cutting in a semicircular shape with variations in pitch ratio and cut diameter. The pitch ratio variations chosen were 4.5, 5.5, and 6.5. The diameter variations chosen were 5 mm, 8 mm, and 11 mm. The results of this study were that the twisted tape semicircular double cut, with a smaller pitch ratio and a larger cut diameter, showed a greater increase in heat transfer and a higher friction factor as well. Next, an earlier study that performed a perforated modification [8] analyzed the thermohydraulic performance of twisted tape with variations of circular and hexagonal perforated shapes. Based on the results of that study, circular perforation yields better heat-exchanger performance.

In engineering applications, the geometry of twisted tape with cutting and perforation is relatively easy to form through a simple manufacturing process, making it widely used for heat-exchanger tubes in industry. Unlike previous studies that investigated cutting and perforation separately, the present study compares semicircular double-cut and circular perforated twisted tapes under identical surface area reduction conditions. This approach enables the influence of geometric modification to be isolated from the effect of insert surface area, providing a more objective evaluation of thermo-hydraulic performance.

METHOD

In this study, the research process is conducted in several stages. The research flowchart illustrates all the processes involved in the research. The research stages are outlined in Figure 1.

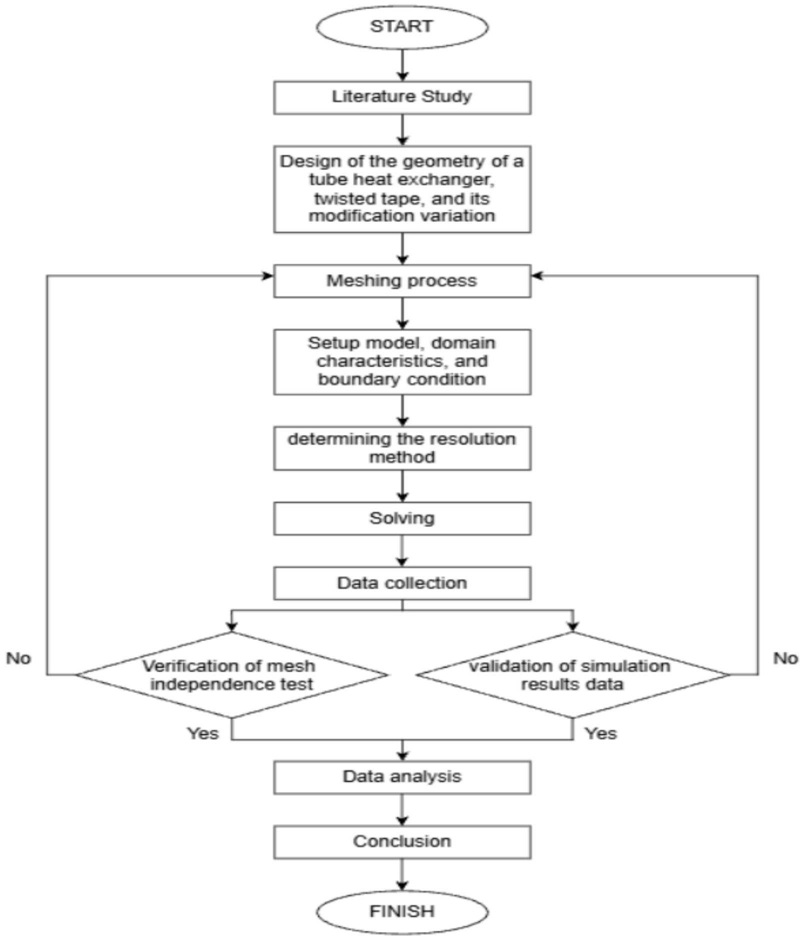

Figure 1. Research Procedure Flowchart.

A. Geometry Modeling

The Geometry Model in the heat exchanger tube simulation consists of two domains: the fluid and solid domains. The fluid domain is a physically bounded volume of space within which fluid flow occurs. The physical representation of the fluid area is a horizontal cylindrical tube measuring 1000 mm in length and 17 mm in diameter. The twisted tape measures 1000 mm in length, has a thickness of 1 mm, a width of 16 mm, and possesses a twist ratio (y/w) of 5. Next, both types of modifications, namely semicircular double-cut and circular perforation, each have a reduced area with a diameter of 8 mm and a pitch distance of 80 mm. The computational domain for the horizontal cylindrical tube with twisted tape and its modifications is shown in Figure 2.

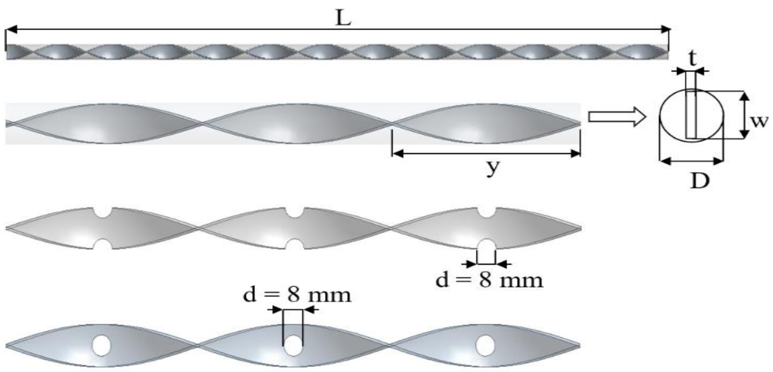

Figure 2. Geometry details. Tube and twisted tape length, dimension details of plain twisted tape, cut diameter of semicircular double cut, and perforated diameter of circular perforated.

Table 1. Detailed information on the tube and twisted tape.

Parameter	Symbol	Dimension (mm)
Tube length	L	1000
Hydraulic diameter	D	17
Twisted tape length	L	1000
Twisted tape wide	w	16
Twisted tape Thickness	t	1
Twisted tape Pitch	y	80

The material used for the twisted tape is stainless steel 304, and the fluid is water. The characteristics of each material are stated in Tables 2 and 3 [9], [10], [11].

Table 2. Material Properties of Stainless Steel 304.

properties	Value
Density	7954,3 Kg/m^3
Thermal conductivity, k	14,924 W/m.K
Specific heat, C_p	473,62 J/Kg.K

Table 3. Material Properties of Water

properties	Value
Density	998,2 Kg/m^3
Thermal conductivity, k	0,6 W/m.K
Specific heat, C_p	4182 J/Kg.K
Dynamic viscosity, μ	0,001003 Kg/m.s

Each modification to the twisted tape, consisting of the semicircular double-cut and the circular perforation, reduces the surface area of the twisted tape by 628 mm^2.

B. Computational Modeling

The study of the heating fluid flow in this research uses the Reynolds-Averaged Navier-Stokes (RANS) technique. To ensure fluid mass conservation throughout the domain, the equations solved include the mass conservation equation (continuity equation) in (1) and the momentum equations for the X-, Y-, and Z-axes in (2), (3), (4). Additionally, the energy equation is applied to both the fluid domain in (5) and the solid domains in (6) [12].

$$\frac{\partial u}{\partial x}+\frac{\partial v}{\partial y}+\frac{\partial w}{\partial z}=0 \tag{1}$$

$$\rho\left(u\frac{\partial u}{\partial x}+v\frac{\partial u}{\partial x}+w\frac{\partial u}{\partial x}\right)=-\frac{\partial p}{\partial x}+\mu\left(\frac{\partial^2 u}{\partial x^2}+\frac{\partial^2 u}{\partial y^2}+\frac{\partial^2 u}{\partial z^2}\right) \tag{2}$$

$$\rho\left(u\frac{\partial v}{\partial y}+v\frac{\partial v}{\partial y}+w\frac{\partial v}{\partial y}\right)=-\frac{\partial p}{\partial y}+\mu\left(\frac{\partial^2 v}{\partial x^2}+\frac{\partial^2 v}{\partial y^2}+\frac{\partial^2 v}{\partial z^2}\right) \tag{3}$$

$$\rho\left(u\frac{\partial w}{\partial z}+v\frac{\partial w}{\partial z}+w\frac{\partial w}{\partial z}\right)=-\frac{\partial p}{\partial z}+\mu\left(\frac{\partial^2 w}{\partial x^2}+\frac{\partial^2 w}{\partial y^2}+\frac{\partial^2 w}{\partial z^2}\right) \tag{4}$$

$$\left(u\frac{\partial T}{\partial x}+v\frac{\partial T}{\partial y}+w\frac{\partial T}{\partial z}\right)=\alpha\left(\frac{\partial^2 T}{\partial x^2}+\frac{\partial^2 T}{\partial y^2}+\frac{\partial^2 T}{\partial z^2}\right) \tag{5}$$

$$\left(\frac{\partial^2 T}{\partial x^2}+\frac{\partial^2 T}{\partial y^2}+\frac{\partial^2 T}{\partial z^2}\right)=0 \tag{6}$$

The following simplifying assumptions were adopted [8]:

- CFD simulation using twisted tape geometry modeling in a three-dimensional (3D) fluid flow domain.
- The movement of the fluid is chaotic, consistent, and cannot be compressed.
- The physical and thermal characteristics of the fluid are considered to remain unchanged by utilizing liquid water.
- A no-slip boundary condition is applied to the tube wall.
- Thermal radiation, material deformation, and gravity are assumed to be negligible.

The K-omega SST (Shear Stress Transport) model was chosen for its advantages in handling strong swirl flow and high pressure gradients caused by the addition of twisted tape inside the tube. This model combines the benefits of the K-epsilon model, which is more stable in the free stream, with the K-omega model, which effectively represents near-wall flow characteristics. Consequently, vortex formations and flow separations can be captured with high accuracy using the K-omega SST model, boundary-layer interactions, and velocity distributions. These advantages play a significant role in producing accurate Nusselt number and friction factor values [13].

C. Mesh Process

The meshing process is performed in the computational domain using ANSYS Fluent 2022 R1. The mesh element method used is a tetrahedral one, applied to each domain. Tetrahedra were chosen because they are flexible in representing complex geometries and are highly compatible with applying inflation layers to walls, which significantly affects the accuracy of the simulation results [14]. The inflation layer is added to capture the fluid flow near the wall, where the velocity and temperature gradients change rapidly. Inflation is applied to the fluid domain. The inflation option used is the first-layer thickness. The first-layer height is determined to achieve y+ = 1 for the k-ω SST model and is adjusted with the Reynolds number [13].

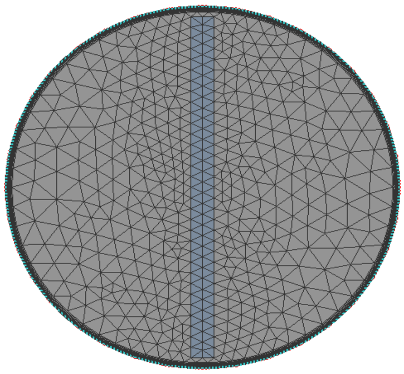

Figure 3. Mesh model of a tube filled with twisted tape.

The size of the mesh elements significantly affects simulation results; mesh verification is necessary to determine an appropriate mesh size while balancing computational efficiency. Mesh verification is performed using the Grid Convergence Index (GCI) Roache method based on Richardson extrapolation to ensure the numerical solution is independent of mesh density [15]. The testing was conducted on a plain tube. The results of the mesh verification testing are shown in Table 4. The mesh refinement ratio sets a restriction on the number of elements in each mesh, as given by (13). Next, the percentage error for each mesh-size refinement is determined using (14). Then, to calculate the probability that the fine and medium meshes change if the mesh is refined further, (15) and (16) can be used. Subsequently, to verify the mesh convergence index, (17) can be used. And to calculate the error between two levels of element counts, (18) is used [16]

$$r = \frac{h_1}{h_2} \tag{7}$$

$$p = \frac{ln\left(\frac{f_3-f_2}{f_2-f_1}\right)}{ln(r)} \tag{8}$$

$$GCI_{fine} = \frac{F_s|\epsilon_{12}|}{(r^p-1)} \tag{9}$$

$$GCI_{coarse} = \frac{F_s|\epsilon_{23}|}{(r^p-1)} \tag{10}$$

$$\frac{GCI_{coarse}}{GCI_{fine}r^p} \approx 1 \tag{11}$$

$$\epsilon = \frac{f_{n+1}-f_n}{f_n} \tag{12}$$

Table 4. Mesh Independent Test Result.

Mesh Category	Fine	Medium	Coarse
Elements	3.528.832	2.758.921	1.806.093
Nu	103,17	101,83	98,93
r		1,12	
p		6,90	
GCI_{fine}		1,39%	
GCI_{coarse}		3,05%	
GCI ratio		1,01	
Error	-	1,30%	2,85%

Based on the results shown in the mesh independence test table, the chosen mesh size is the medium mesh. The selection of this mesh size was based on the GCI ratio result of 1, considering computational efficiency.

D. Boundary condition

Numerical analysis using CFD software (ANSYS Fluent) was conducted on the geometry of a heat exchanger tube with a twisted tape inserted. This study performed a comparative analysis of two types of modifications to the twisted tape, namely semicircular double-cut and circular perforated, to reduce the twisted tape surface area to the same magnitude. The simulation uses the K-ω SST model, chosen for its superior ability to capture flow separation and near-wall gradients. The fluid used in the simulation is liquid water at 20 Celsius entering the tube inlet. Convective heat transfer occurs within the fluid when a heat flux of 1200 W/m2 is provided. The Nusselt number (Nu) is the ratio of convective heat transfer to the fluid's natural conduction. Then, to determine the pressure drop, a static gauge is set to 0 Pa at the outlet. By establishing this reference value, the inlet-side pressure reading represents the pressure difference along the tube.

E. Data Collection and Data Analysis

The case in this study uses varying Reynolds numbers to analyze flow phenomena with different speeds in each simulation. The Reynolds number is expressed as:

$$Re = \frac{\rho . D . \bar{v}}{\mu} \tag{13}$$

Where *Re* denotes a dimensionless value indicating the Reynolds number, ρ represents the density of the fluid measured in Kg/m³, refers to the average flow velocity of the incoming fluid, expressed in m/s, *D* refers to the diameter of the tube measured in meters, and μ signifies the dynamic viscosity of the fluid with units of Kg/m.s. [17].

The thermo-hydraulic analysis of fluid flow for each twisted-tape variation is conducted using the friction factor and Nusselt number values obtained from CFD simulations. The Nusselt number is expressed as:

$$Nu = \frac{D.h}{k} \tag{14}$$

Where the Nusselt number, commonly called *Nu*, serves as a dimensionless metric indicating the relationship between convective heat transfer at the fluid-solid interface; k is the fluid's thermal conductivity expressed in W/m² K; and *D* is the tube's internal diameter or hydraulic diameter. Measured in meters, and *h* symbolizes the convective heat transfer coefficient. [18].[19]. is expressed as [20]:

$$h = \frac{Q}{T_w - T_b} \tag{15}$$

In this context, *h* represents the convective heat transfer coefficient, measured in W/m^2.K, while Q denotes the heat flow rate, also measured in W/m^2. The variable T_w signifies the mean temperature of the whole wall surface that directly interacts with the fluid, given in K, and T_b is the bulk temperature expressed as:

$$T_b = \frac{T_{in} - T_{out}}{2} \tag{16}$$

T_b is the bulk temperature in K; T_{in} and T_{out} represent the fluid's temperatures at the inlet and outlet in K [21] [22]. The friction factor is expressed as:

$$f = \frac{\Delta p}{\left(\frac{L}{D}\right)\left(\frac{\rho . u^2}{2}\right)} \tag{17}$$

Where f is the friction factor, a dimensionless number that indicates the magnitude of the frictional force occurring between the working fluid and the tube wall, causing a reduction in fluid energy and resulting in a pressure drop (Δp). Δp is the decrease in pressure, quantified in Pa; L is the length of the heated tubing, measured in m; and D is the internal diameter of the tube (inner tube), measured in m. The fluid's average velocity, expressed in m/s, is denoted by u, while its density, expressed in kg/m³, is represented by ρ [23] [24].

Then, the evaluation of the heat exchanger's performance is carried out by employing the Performance Evaluation Criteria (PEC) formula, which is expressed as:

$$PEC = \frac{\left(Nu/_{Nu_p}\right)}{\left(f/_{f_p}\right)^{1/3}} \tag{18}$$

Where *PEC* is a dimensionless number that measures the balance between the benefits gained from increased heat transfer and the losses due to pressure drop, *Nu* is a dimensionless number that represents the Nusselt number in the modified heat exchanger, and Nu_p is a dimensionless number that represents the Nusselt number in the unmodified heat exchanger, in this case, a plain tube. Meanwhile, the modified heat exchanger's friction factor is denoted by f, while the unmodified heat exchanger's friction factor is denoted by f_p (in this case, a plain tube) [25]-[26]

RESULT AND DISCUSSION

A. Validation

Validation of the simulation is necessary to ensure the precision of the results. During this phase, the outcomes generated by the simulation are evaluated against experimental data and analytical equations. Validation is conducted on a plain tube. Two values from the simulation results are used for validation: the Nusselt number and the friction factor. These two values will be compared with the experimental results and analytical equations. The analytical equations used to validate the Nusselt number are the Dittus-Boelter and Gnielinski equations [11]-[27]

The Dittus-Boelter equation

$$Nu = 0.023Re^{0.8}Pr^{0.4} \tag{19}$$

Gnielinski equation

$$Nu = \frac{(f/8)(Re-1000)Pr}{1+12.7(f/8)^{1/2}(Pr^{2/3}-1)}\left[1+\left(\frac{d}{L}\right)^{2/3}\right] \tag{20}$$

Where P_r is the Prandtl number, expressed as:

$$Pr = \frac{\mu C_p}{k} \tag{21}$$

Where k is the fluid's thermal conductivity expressed in W/m² K, C_p is specific heat with units of J/Kg.K, and μ is the fluid's dynamic viscosity with values of Kg/m.s. [28]. Meanwhile, the analytical equations used to validate the friction factor are the Blasius and Petukhov equations [11][30].

Blasius equation

$$f = 0.316Re^{-0.25} \tag{22}$$

Petukhov equation

$$f = (1.82log\ Re - 1.64)^{-2} \tag{23}$$

For the validation test of the experimental results, based on the experimental research conducted by Toygun Dagdevir and Veysel Ozceyhan [11]. The simulation results are shown in Figure 4 and are validated against the analytical equation and experimental results.

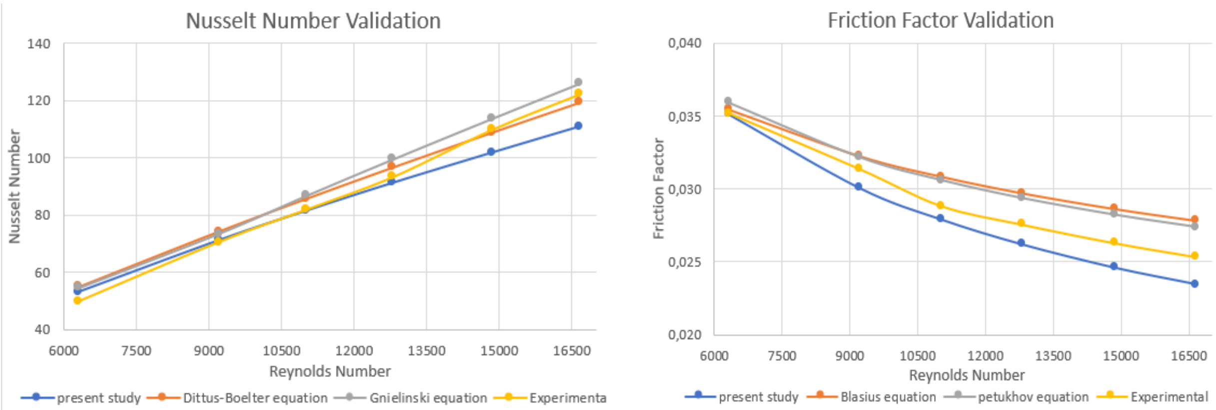

Figure 4. Nusselt Number Validation and Friction Factor Validation.

In Figure 4, the mean relative error of the Nusselt number validation against the Dittus-Boelter equation is 5.60%, against the Gnielinski equation is 7.95%, and against the experimental results is 4,02%. Meanwhile, the validation of the friction factor has a mean relative error of 9.75% against the Blasius equation, 9.21% against the Petukhov equation, and 4,36% against experimental results. The consistency of simulation results with experimental data and numerical equations indicates an adequate level of reliability; thus, the model validation has been verified, and the discussion of the next configuration may proceed.

B. Nusselt Number

Figure 5 presents the Nusselt number (Nu) values for a smooth tube and three twisted tape configurations: smooth twisted tape, double-cut semicircular, and circular perforation. The Nusselt number value in all configurations will consistently increase as the Reynolds number increases. This is because higher Reynolds numbers have higher velocities and greater turbulence. The average percentage increase in Nu for each version of the twisted tape relative to the plain tube is 36.64% for the plain twisted tape (PTT), 40.94% for the double semicircular twisted tape (TT SCDC), and 36.95% for the perforated twisted tape. In a smooth pipe, heat transfer is still very limited and occurs only in the region near the wall. This is caused by the flow being in a free stream, so the convective heat transfer occurs only by heat conduction, without any effort to disturb the fluid flow (natural convection). The insertion of a twisted tape into a plain tube enhances heat exchange, which can improve fluid mixing. Additionally, the addition of a twisted tape can create a swirling flow that generates a centrifugal force, continuously pushing fluid particles towards the tube wall. This results in much more efficient convective heat transfer than in a smooth pipe, as evidenced by a significant increase in the Nusselt number for the pipe with twisted tape. The modifications made to the twisted tape result in changes to the flow. The use of circular perforated tape enhances heat transfer by inducing bypass flow and turbulence around the holes, increasing the flow time and thereby maximizing heat transfer. Then, the use of semicircular double-cut tape increases heat transfer by enhancing turbulence in the flow on both edges of the twisted tape that are very close to the pipe wall. This causes more massive fluid mixing and faster, more effective heat transfer because the added turbulence effect occurs near the wall. The difference in the location of the turbulence effect results in a higher Nusselt number for the semicircular double-cut modification compared to the circular perforated one, where the turbulence effect is added around holes far from the pipe wall.

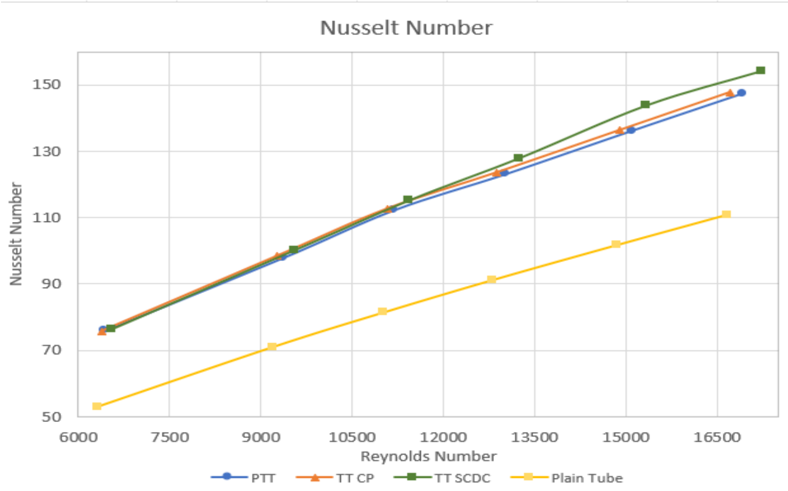

Figure 5. Simulation result of Nusselt number with varied Reynolds number for plain tube, PTT, TT SCDC, and TT CP.

C. Friction Factor

Figure 6 shows the friction factor (f) values for a plain tube and three twisted-tape configurations: plain, semicircular double-cut, and circular perforated. The friction factor in all configurations will consistently decrease as the Reynolds number increases because higher speeds reduce the relative impact of viscosity. The average percentage increase in the friction factor for every variation of twisted tape compared to the plain tube is 232.26% for plain twisted tape (PTT), 253.46% for semicircular double-cut twisted tape (TT SCDC), and 239.96% for circular perforated twisted tape (TT CP). In a smooth pipe, the very low friction factor indicates minimal flow resistance because no elements can disrupt the flow. Incorporating twisted tape into the smooth tube increases the resistance between the liquid and the tube wall and the surface of the twisted tape, resulting in a greater pressure drop. The vortex flow generated by twisted tape produces a centrifugal force that continuously pushes fluid particles toward the tube wall, thereby increasing friction.

The double-cut and circular-perforated modifications to twisted tape can increase the friction factor. The circular-perforated modification exhibits a higher friction factor than plain twisted tape. This is due to additional resistance that causes turbulence near the holes, creating vortices and increasing friction between the fluid and the twisted tape surface around the holes. The addition of the semicircular double-cut modification yields the highest friction factor among all configurations, due to flow resistance that generates high vortex intensity at both edges of the twisted tape in direct contact with the pipe wall. This results in friction not only between the fluid and the twisted-tape surface but also in increased friction between the fluid and the pipe wall.

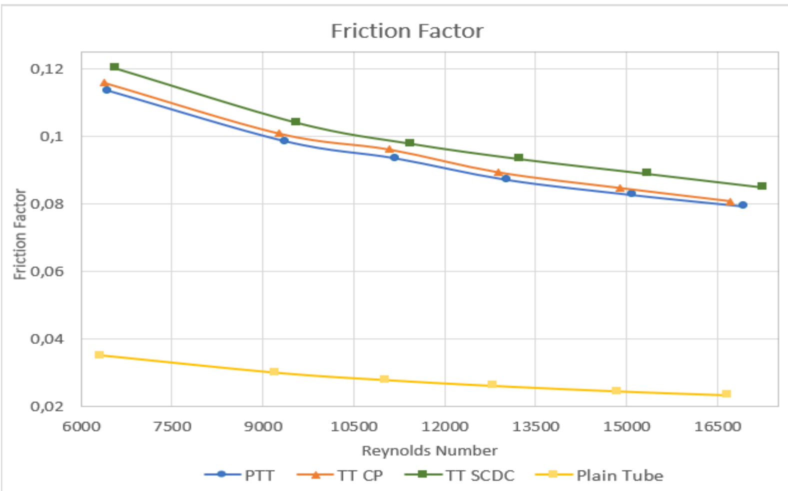

Figure 6. Simulation result of the friction factor with varied Reynolds number for plain tube, PTT, TT SCDC, and TT CP.

D. Performance Evaluation Criteria (PEC)

Figure 7 presents the evaluation of hydraulic performance based on the PEC equation. The PEC provides a comparative evaluation of hydraulic performance for each modification of the helical tape against the plain tube. Inserting twisted tape into the heat exchanger tube can enhance heat transfer but also increase the fluid friction factor, resulting in a pressure drop. Therefore, a thermohydraulic performance evaluation is necessary to assess the balance of benefits and drawbacks resulting from the addition of twisted tape. The PEC graph shows that the PEC value for all configurations decreases as the Reynolds number increases. This indicates that the friction factor becomes more dominant compared to the Nusselt number as the Reynolds number increases.

The analysis shows that the semicircular-double-cut twisted tape modification has a higher PEC than all other configurations, reflecting a higher heat-transfer-to-friction-factor ratio than the circular perforated and plain twisted tape modifications. Meanwhile, the circular-perforated modification yields a lower PEC value than the plain twisted tape, indicating that the addition of holes in the twisted tape makes the friction factor more dominant over heat transfer than in the plain twisted tape. The plain twisted tape has an average PEC value of 0.9158. The modified half-circle twisted tape with two cuts yields an average PEC value of 0.9254, while the circular perforated twisted tape yields an average PEC value of 0.9110. Data from the performance evaluation of all twisted tape modification configurations consistently yield PEC values below 1 (PEC < 1) within the Reynolds number range of 6000 to 16500. This indicates that within the Reynolds number range of 6000 to 16500, inserting twisted tape into the tube can reduce the heat exchanger's efficiency, as the increase in the Nusselt number is smaller than the increase in the friction factor.

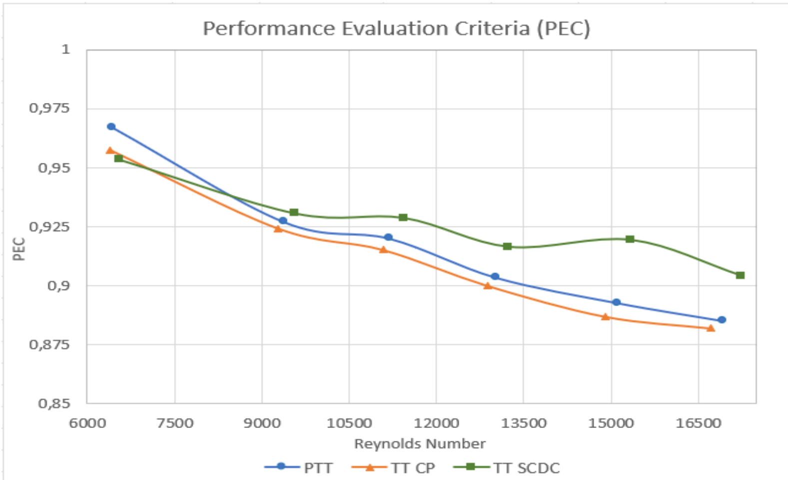

Figure 7. Simulation result of the PEC with varied Reynolds number for plain tube, PTT, TT SCDC, and TT CP.

E. Temperature Contour

The temperature contours are presented using CFD Post after the simulation is completed. The contour in the smooth tube, where there are no disturbances in the fluid flow, shows that the fluid temperature distribution is uneven and that heat propagates only near the walls, resulting in a characteristic layered structure. The dark blue contours indicate that the fluid far from the wall remains relatively cold. Meanwhile, inside the tube that has been inserted with twisted tape, the temperature contour color at the core of the fluid flow is light blue, indicating that the higher temperature distribution near the wall has reached the core of the fluid flow and has spread throughout the fluid flow, making the heat transfer process more efficient. The addition of twisted tape generates turbulence and forces the flow to continually approach the wall, thereby thinning the thermal boundary layer and increasing fluid mixing.

The temperature contour in the circular perforated configuration shows bypass flow through the holes, creating turbulence from the resulting flow disturbance. The temperature contour shows light colors in the configuration, indicating that the heat has spread throughout the fluid. In addition, the thermal boundary layer near the pipe wall appears thinner than that of plain twisted tape due to the additional turbulence caused by the holes, which thins the fluid's boundary layer near the wall. Meanwhile, the temperature contour in the semicircular double-cut configuration is light blue and brighter than in other configurations, indicating that heat near the wall has been evenly distributed throughout the fluid. The addition of a double-cut along the edge of the twisted tape has increased turbulence and helped significantly thin the thermal boundary layer. This occurs because the turbulence is near the pipe wall, making the thinning of the thermal boundary layer more effective. The hot fluid particles near the wall will quickly transfer heat to the entire fluid.

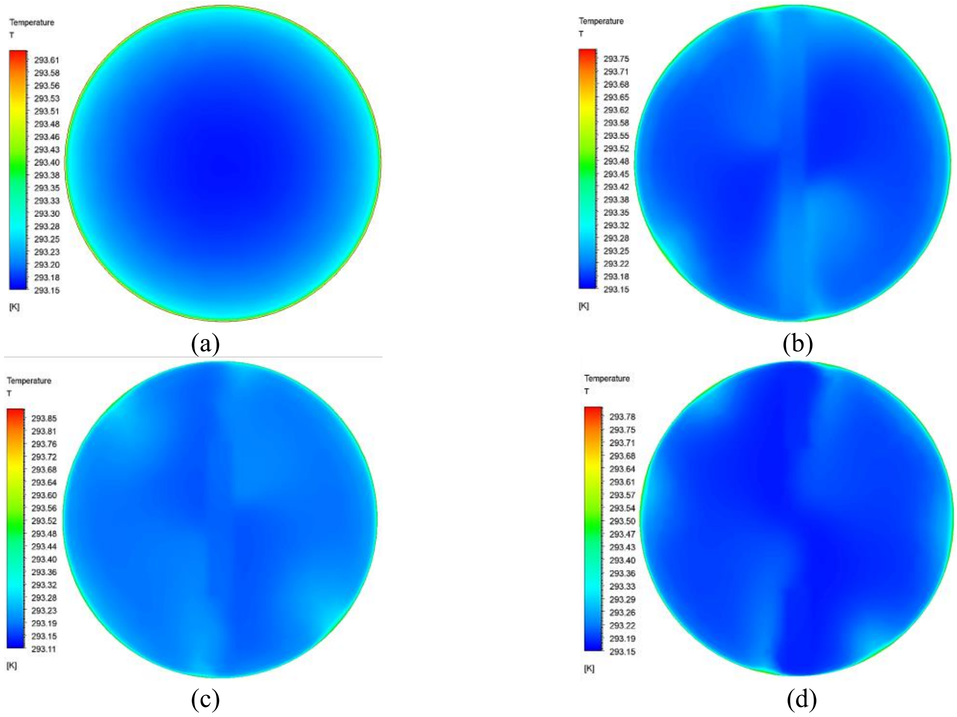

Figure 8. Temperature contour for (a) plain tube, (b) plain twisted tape, (c) semicircular double-cut twisted tape, and (d) circular perforated twisted tape at Re=13000 and a distance of 520 mm from the inlet.

F. Velocity Contour

The velocity contours in the smooth tube and the variations resulting from the modification of the twisted tape are presented using CFD Post after the simulation is completed. In the smooth tube, the velocity contour profile exhibits a standard turbulent flow pattern, with the highest velocity (red) concentrated in the core of the flow. However, as it approaches the tube wall surface, the velocity gradually decreases due to viscous effects. The absence of disturbances in the fluid flow causes the thermal boundary layer to remain structured, indicating that heat has not yet spread evenly throughout the fluid. When the twisted tape is added to the tube, the fluid velocity near the tube wall increases due to the centrifugal force generated by the vortex flow. This disturbance continuously pushes the fluid towards the wall, disrupting the boundary layer structure and thereby enhancing heat transfer performance, as the exchange of fluid particles becomes more intense. The heat is now more evenly distributed, as evidenced by the change in velocity contour color from red in the smooth pipe to orange in the pipe with the twisted tape inserted. The fluid velocity increases due to turbulence generated by the insertion of the twisted tape.

In the circular-perforated modification, the flow velocity contour becomes more complex. There is flow passing through the holes, as evidenced by the slightly bluish contour in the hole area. In the presence of holes, turbulence increases, and the intensity of interaction between the fluid near the wall and the flow core increases. This results in more uniform fluid mixing than plain twisted tape. However, the velocity produced by the circular-perforated modification is slightly lower than that of the plain twisted tape due to the perforations obstructing part of the fluid flow. The use of semicircular double cut modifications can increase fluid flow velocity. This is because the double cut offers lower resistance, as the large cuts on the tape create a more continuous flow path, minimizing physical resistance and wake effects. Visually, the velocity contours show a wider distribution of orange-colored contours than those of plain twisted tape. This indicates improved interaction between the fluid near the wall and the fluid in the core flow, enabling an uninterrupted path and thereby enhancing heat transfer.

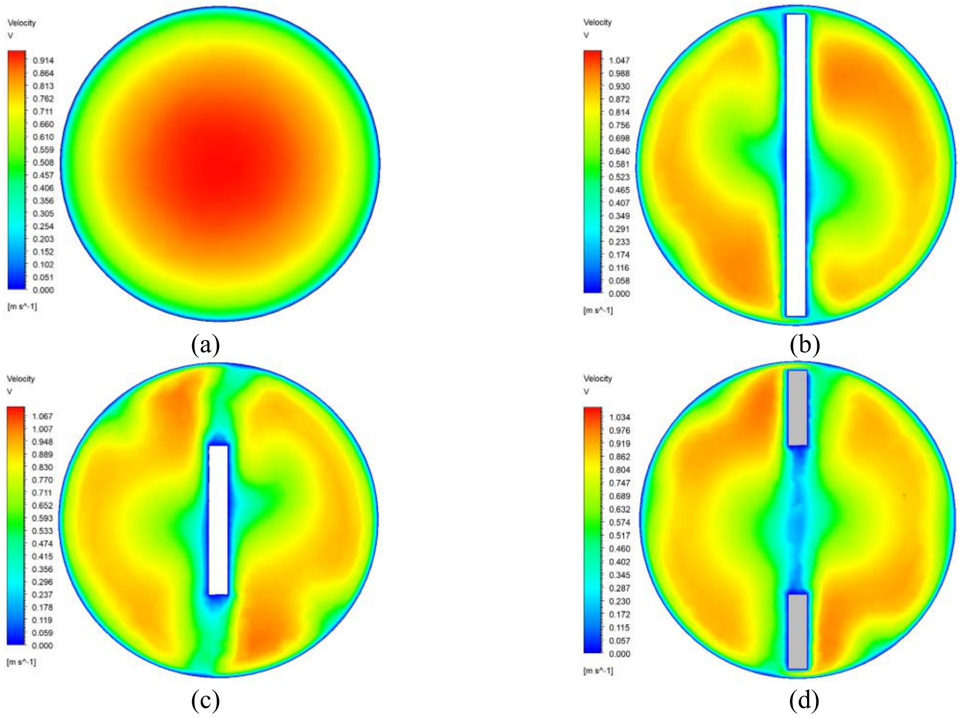

Figure 9. Velocity contour for plain tube, plain twisted tape, semicircular double-cut twisted tape, and circular perforated twisted tape at Re=13000 and distance 520 mm from the inlet.

CONCLUSION

This research has evaluated the thermohydraulic performance of two types of twisted tape modifications, namely semicircular double-cut twisted tape and circular perforated twisted tape, using Computational Fluid Dynamics (CFD) simulations in ANSYS Fluent with the k-ω SST turbulence model, while keeping the surface area of the twisted tape in each modification constant. The validation results show that the numerical model has a high level of accuracy compared to experimental data and analytical correlations. Analysis shows that the semicircular double-cut modification yields the largest increase in heat transfer, with an average Nusselt number increase of 40.94%, but also causes the largest increase in friction factor, by 253.46%. Meanwhile, evaluation using Performance Evaluation Criteria (PEC) indicates that all configurations have PEC values below 1, suggesting that the increase in heat transfer has not yet compensated for the energy loss due to pressure drop in the Reynolds number range of 6000 to 16500. Nevertheless, the semicircular double-cut configuration yielded the highest PEC among the configurations, indicating better thermohydraulic performance. The main implication of this research is that the distribution and location of turbulence generation resulting from modifications to the twisted-tape geometry have a greater impact on thermal-hydraulic performance than merely reducing the insert's surface area. These findings make an important contribution to the development of passive heat-transfer enhancement design strategies, particularly for optimizing the geometry of twisted tape in industrial heat exchanger applications, emphasizing the need for a balance between increased heat transfer and pressure-drop penalties.

REFERENCE

[1] S. Bhattacharyya and D. K. Vishwakarma, "Mixed and forced convection heat transfer and pressure drop in inclined tube with twisted tape in transition flow," *Sci. Rep.*, vol. 15, no. 1, Dec. 2025.

[2] J. Heeraman, R. Kumar, P. K. Chaurasiya, H. Ivanov Beloev, and I. Krastev Iliev, "Experimental evaluation and thermal performance analysis of a twisted tape with dimple configuration in a heat exchanger," *Case Studies in Thermal Engineering*, vol. 46, Jun. 2023.

[3] Y. Du *et al.*, "Heat Transfer Intensification in a Heat Exchanger Tube with Continuous V-Rib Twisted Tapes Installed," *Applied Sciences (Switzerland)*, vol. 15, no. 10, May 2025.

[4] M. K. Diwaker and A. Kumar, "Thermo-Hydraulic Performance of Tube Type Heat Exchanger with Semi-Circular Cut Twisted Tape Insert: A Numerical Exploration," *Journal of Heat and Mass Transfer Research*, vol. 10, no. 1, pp. 159–170, Jun. 2023.

[5] A. Bouregueba, A. Begag, R. Saim, and M. A. Kherrafi, "Heat Transfer Enhancement in a Heat Exchanger Tube Using Twisted Tapes with Circular and Hexagonal Perforations," *International Journal of Thermodynamics*, vol. 28, no. 3, pp. 187–195, Sep. 2025.

[6] K. Deshmukh, S. Karmare, and P. Patil, "Experimental investigation of convective heat transfer inside tube with stable plasmonic TiN nanofluid and twisted tape combination for solar thermal applications," *Heat and Mass Transfer/Waerme- und Stoffuebertragung*, vol. 59, no. 8, pp. 1379–1396, Aug. 2023.

[7] G. Liu, C. Yang, J. Zhang, H. Zong, B. Xu, and J. Y. Qian, "Internal flow analysis of a heat transfer enhanced tube with a segmented twisted tape insert," *Energies (Basel).*, vol. 13, no. 1, Jan. 2020.

[8] S. R. Nashee, "Numerical Simulation of Heat Transfer Enhancement of a Heat Exchanger Tube Fitted with Single and Double-Cut Twisted Tapes," *International Journal of Heat and Technology*, vol. 42, no. 3, pp. 1003–1010, Jun. 2024.

[9] S. Manova *et al.*, "Experimental investigation on the heat transfer characteristics of nanofluids in a cylindrical heat exchanger tube using quad-structured vortex generator with semi-perforations," *Results in Engineering*, vol. 27, Sep. 2025.

[10] H. W. Ayoob *et al.*, "The thermal-flow performance of water-Al2O3 nanofluid flow in an elliptical duct heat exchanger equipped with two rotating twisted tapes," *Case Studies in Chemical and Environmental Engineering*, vol. 11, Jun. 2025.

[11] T. Dagdevir and V. Ozceyhan, "An experimental study on heat transfer enhancement and flow characteristics of a tube with plain, perforated and dimpled twisted tape inserts," *International Journal of Thermal Sciences*, vol. 159, Jan. 2021.

[12] S. Edhy Sofyan, Z. Maulana, A. Tamlicha, and M. Syaukani, "Development of CFD simulation model of earth air heat exchanger for space cooling of a 36 m 2 house in tropical climate Banda Aceh, Indonesia," *Disseminating Information on the Research of Mechanical Engineering-Jurnal Polimesin*, vol. 21, no. 2, 2023.

[13] R. Cabello, A. E. Plesu Popescu, J. Bonet-Ruiz, D. Curcó Cantarell, and J. Llorens, "Heat transfer in pipes with twisted tapes: CFD simulations and validation," *Comput. Chem. Eng.*, vol. 166, Oct. 2022.

[14] P. Aziziyan, M. M. Sadeghi Azad, and C. Rahim, "Computational Investigation of Flow Dynamics in Multi-Channel Twisted Tape Heat Exchanger with Rectangular Cuts," 2024.

[15] P. J. Roache, "QUANTIFICATION OF UNCERTAINTY IN COMPUTATIONAL FLUID DYNAMICS," 1997.

[16] M. Lee, G. Park, C. Park, and C. Kim, "Improvement of Grid Independence Test for Computational Fluid Dynamics Model of Building Based on Grid Resolution," *Advances in Civil Engineering*, vol. 2020, 2020.

[17] I. Roswandi, A. S. Pamitran, M. Juarsa, and A. A. Budiman, "Experimental investigation of the impact of non-uniform pipe diameters on natural circulation and dimensionless flow in in a rectangular loop," 2024.

[18] V. Roda-Casanova and C. M. C. G. Fernandes, "A comparison of analytical methods to predict the bulk temperature in polymer spur gears," Jul. 01, 2022, *Elsevier Ltd*.

[19] M. K. Sahu, M. Kharub, and M. M. Matheswaran, "Nusselt Number and Friction Factor Correlations Development for Arc-Shape Apex Upstream Artificial Roughness in Solar Air Heater," Dec. 30, 2021.

[20] J. W. Elliott, M. T. Lebon, and A. J. Robinson, "Optimising integrated heat spreaders with distributed heat transfer coefficients: A case study for CPU cooling," *Case Studies in Thermal Engineering*, vol. 38, Oct. 2022.

[21] A. S. Kurhade *et al.*, "Performance Analysis of Corrugated Twisted Tape Inserts for Heat Transfer Augmentation," *Journal of Advanced Research in Fluid Mechanics and Thermal Sciences*, vol. 121, no. 2, pp. 192–200, Sep. 2024.

[22] C. Pedano-Medina, P. Petagna, and S. Gleissle, "Effects of inlet temperature and pressure in sCO 2 heat transfer in a 1 mm diameter horizontal tube." [Online]. Available: https://ssrn.com/abstract=6274890

[23] Y. H. Assaf, A. Akroot, K. Alnamasi, and M. A. Ismail, "Investigation of heat transfer performance in heat exchangers using hybrid nanofluids and twisted tape inserts with fixed special rings," *Sci. Rep.*, vol. 15, no. 1, Dec. 2025.

[24] P. K. Chaurasiya, J. Heeraman, S. K. Singh, T. N. Verma, G. Dwivedi, and A. K. Shukla, "Exploring the combined influence of primary and secondary vortex flows on heat transfer enhancement and friction factor in a dimpled configuration twisted tape with double pipe heat exchanger using SiO2 nano fluid," *International Journal of Thermofluids*, vol. 22, May 2024.

[25] W. Chammam *et al.*, "Estimation of heat transfer coefficient and friction factor with showering of aluminum nitride and alumina water based hybrid nanofluid in a tube with twisted tape insert," *Sci. Rep.*, vol. 13, no. 1, Dec. 2023.

[26] S. A. Marzouk, M. M. Abou Al-Sood, E. M. S. El-Said, M. M. Younes, and M. K. El-Fakharany, "A comprehensive review of methods of heat transfer enhancement in shell and tube heat exchangers," Aug. 01, 2023, *Springer Science and Business Media B.V.*

[27] M. Dostál, K. Petera, and S. Solnař, "Gnielinski's correlation and a modern temperature-oscillation method for measuring heat transfer coefficients," *EPJ Web Conf.*, vol. 269, p. 01009, 2022.

[28] M. S. Islam, M. R. Kabir, and M. A. Islam, "Numerical Analysis of Porous Twisted Tape Influence on Heat Transfer Characteristics in Double Tube Heat Exchanger."

[29] C. P. Tzanos and B. Dionne, "Computational Fluid Dynamics Analyses of Lateral Heat Conduction, Coolant Azimuthal Mixing and Heat Transfer Predictions in a BR2 Fuel Assembly Geometry," May 2011. [Online]. Available: www.anl.gov.